INFECTION AND IMMUNITY, Jan. 2005, p. 403–412 Vol. 73, No. 1
0019-9567/05/$08.00+0 doi:10.1128/IAI.73.1.403–412.2005

Chemokine Expression in the Monocytic Cell Line THP-1 in Response to Purified Shiga Toxin 1 and/or Lipopolysaccharides

Lisa M. Harrison,† Christel van den Hoogen, Wilhelmina C. E. van Haaften, and Vernon L. Tesh*

Department of Medical Microbiology and Immunology, Texas A&M University System Health Science Center, College Station, Texas

Received 25 June 2004/Returned for modification 14 September 2004/Accepted 23 September 2004

Infections with Shiga toxin (Stx)-producing bacteria are associated with bloody diarrhea and postdiarrheal sequelae, including hemolytic uremic syndrome and central nervous system (CNS) abnormalities. Stx-induced intestinal, renal, and CNS vascular lesions may involve a localized production of proinflammatory cytokines in target organs, as tumor necrosis factor-α (TNF-α) and interleukin-1β (IL-1β) up-regulate Stx receptor globotriaosylceramide (Gb_3) expression on vascular endothelial cells. However, leukocyte recruitment to injured sites may also exacerbate vascular damage. A cytokine macroarray analysis of transcripts derived from macrophage-like THP-1 cells treated with Stx1, lipopolysaccharides (LPS), or both demonstrated a consistent up-regulation of *TNF*-α, *IL-1*β, and four genes encoding the chemokines interleukin-8 (IL-8), macrophage inflammatory protein-1α (MIP-1α), MIP-1β, and growth-related oncogene beta (GRO-β). Real-time PCR analysis verified the macroarray results. Northern blot analyses after the addition of the transcriptional inhibitor actinomycin D revealed increased IL-8 mRNA stability in THP-1 cells treated with Stx1 or Stx1 plus LPS. Finally, enzyme-linked immunosorbent assay data for Stx1- plus LPS-treated cells demonstrated a poor correlation between IL-8, MIP-1α, MIP-1β, and GRO-β mRNA levels and protein production, indicating a posttranscriptional regulatory effect. Our data suggest that in response to Stx1 and LPS, macrophages may be a source of chemokines that promote tissue damage through leukocyte recruitment and activation.

Infections with *Shigella dysenteriae* serotype 1 and Shiga toxin (Stx)-producing *Escherichia coli* (STEC) may result in bloody diarrhea and the subsequent development of life-threatening sequelae, including acute renal failure and neurological abnormalities (31). The acute renal failure caused by Stxs is referred to as hemolytic uremic syndrome (HUS) and is characterized by thrombotic microangiopathy, hemolytic anemia with schistocytosis, and thrombocytopenia (34). Similar vascular lesions may occur in the brain, leading to lethargy, disorientation, paralysis, seizures, coma, and death (39). The pathogenesis of bloody diarrhea caused by Stx-producing bacteria is multifactorial; however, Stxs appear to be important contributory virulence factors in hemorrhagic colitis, acting to damage capillaries serving the colon (5). Stx-mediated damage to intestinal blood vessels may create the means of access for toxins and other bacterial constituents, such as lipopolysaccharides (LPS), into the bloodstream. In contrast to intestinal disease, Stxs are essential for the development of HUS and neurological complications, as many of the histopathological features of renal and central nervous system (CNS) vascular damage seen in humans can be reproduced in animals after the administration of purified Stxs (reviewed in reference 26).

Stxs are AB_5 holotoxins, possessing a single, enzymatically active A subunit in noncovalent association with five B subunits (8). The Stx family consists of the prototypical Shiga toxin expressed by *S. dysenteriae* serotype 1 and Shiga toxin 1 (Stx1) and Stx2 produced by STEC. Several Stx1 and Stx2 sequence variants have been characterized (29). The B subunits form a pentameric ring and mediate toxin binding to the glycolipid receptor globotriaosylceramide (Gb_3) (17, 18, 20). After internalization, Stxs undergo retrograde transport through the Golgi apparatus to reach the endoplasmic reticulum and the nuclear membrane (19, 36). The endoplasmic reticular membrane is thought to be the site of translocation of a 27-kDa fragment of the A subunit into the cytoplasm. The *N*-glycosidase activity of the A-subunit fragment cleaves a specific adenine residue from the 28S rRNA of eukaryotic ribosomes, thereby blocking peptide elongation and inhibiting protein synthesis (3, 37).

Studies utilizing human endothelial cells have shown that Stxs possess minimal direct cytotoxicity for cultured cells (28, 44). In the presence of the proinflammatory cytokine tumor necrosis factor alpha (TNF-α) or interleukin-1β (IL-1β), however, Stx-mediated endothelial cell cytotoxicity increases significantly (22, 44), and TNF-α and IL-1β were shown to up-regulate the expression of Gb_3 on endothelial cells (33, 48, 51). Endothelial cells do not appear to be a major source of TNF-α or IL-1β synthesized in response to Stxs (42). Our studies indicate that the innate immune response triggered by the interaction of Stxs with macrophages may play a key role in the pathogenesis of HUS and CNS pathology by providing the cytokines necessary to sensitize vascular endothelial cells to the action of the toxins (32). Chemokines may also play a role in the pathogenesis of disease caused by Stx-producing bacteria. Neutrophil transmigration into the intestinal lumen is a hall-

* Corresponding author. Mailing address: Department of Medical Microbiology and Immunology, 407 Reynolds Medical Building, Texas A&M University System Health Science Center, College Station, TX 77843-1114. Phone: (979) 845-1313. Fax: (979) 845-3479. E-mail: tesh@medicine.tamu.edu.

† Present address: Department of Microbiology and Immunology, University of Maryland School of Medicine, Baltimore, MD 21201.

mark of some inflammatory diseases of the gastrointestinal tract, including those mediated by *S. dysenteriae* serotype 1 and STEC (40). Purified Stxs have been shown to directly induce the expression of the neutrophil chemoattractant interleukin-8 (IL-8 or CXCL8) by human intestinal epithelial cells (45, 53). The treatment of intestinal epithelial cells with Stx1 results in the stabilization of IL-8 mRNA, which may lead to prolonged IL-8 production and secretion and increased neutrophil infiltration into the intestine (46). Finally, IL-8 and monocyte chemoattractant protein 1 (MCP-1 or CCL2) have been detected in the urine and sera of some HUS patients (50), suggesting that chemokines are expressed after the hematogenous dissemination of Stxs. The role in pathogenesis of chemokines expressed by macrophages in response to Stxs and LPS has not been extensively studied. Nonadherent human blood monocytes were shown to express IL-8 in response to treatment with Stxs (49), but nonadherent monocytes may not fully reproduce the activities of tissue macrophages populating the lamina propria, kidneys, and CNS. The human monocytic cell line THP-1 may be differentiated to a mature macrophage-like state, and these cells possess many of the physiological properties of primary monocyte-derived macrophages (1). For this study, we utilized macroarrays spotted with 268 cytokine and chemokine cDNAs to investigate the chemokine response of differentiated, macrophage-like THP-1 cells treated with purified Stx1, LPS, or both. Real-time PCR and Northern blot analyses were used to confirm the macroarray results and to examine the kinetics of IL-8 transcript expression, respectively. We examined the relative stabilities of IL-8 transcripts induced by Stx1, LPS, or both. Finally, we examined the synthesis and secretion of chemokines by Stx1- and/or LPS-treated THP-1 cells.

MATERIALS AND METHODS

Cells and toxins. The human myelogenous leukemia cell line THP-1 (47) was obtained from the American Type Culture Collection, Rockville, Md. The cells were maintained in RPMI 1640 (Invitrogen, Carlsbad, Calif.) supplemented with 10% fetal bovine serum (HyClone Laboratories, Logan, Utah), penicillin (100 U/ml), and streptomycin (100 μg/ml) at 37°C in 5% CO_2 in a humidified incubator. Stx1 was expressed from the recombinant *E. coli* DH5α(pCKS112) strain, which harbors a plasmid containing the *stx1* operon under control of a thermoinducible promoter (43). Stx1 in bacterial lysates was purified by sequential ion-exchange, chromatofocusing, and immunoaffinity chromatography. Prior to use, Stx1 preparations were shown to contain <0.1 ng of endotoxin/ml by use of a *Limulus* amoebocyte lysate assay. Purified LPS derived from *E. coli* O111:B4 was purchased from Sigma Chemical Co. (St. Louis, Mo.). *E. coli* O111 strains may be STEC strains that are capable of causing outbreaks of hemorrhagic colitis or HUS.

Macrophage differentiation and stimulation. The mature macrophage-like state was induced by treating THP-1 cells (10^6 cells per ml) for 48 h with 50 ng of phorbol 12-myristate 13-acetate (PMA; Sigma Chemical Co.)/ml in culture dishes. Differentiated, plastic-adherent cells were washed twice with cold, sterile Dulbecco's phosphate-buffered saline (Sigma) and then incubated with fresh medium without PMA but containing 10% fetal bovine serum, penicillin (100 U/ml), and streptomycin (100 μg/ml). The medium was changed every 24 h for the next 3 days. Experiments were performed on the fourth day after PMA removal. For all experiments, differentiated cells were treated with Stx1 (400 ng/ml), LPS (200 ng/ml), or Stx1 plus LPS (400 and 200 ng/ml, respectively) for various times. We previously demonstrated that these stimulant doses produced maximal cytokine protein secretion in differentiated THP-1 cells in vitro (32). The amount of Stx that is necessary to cause systemic disease in humans is unknown, but the Stx1 dose used in these experiments represents approximately 4×10^5 50% cytotoxic doses for Vero cells and 1 50% lethal dose for CD-1 mice (43). The infusion of 200 to 280 ng (3 to 4 ng/kg of body weight) of LPS into human volunteers induced hemodynamic changes and elevated TNF-α levels in sera (27).

TABLE 1. Real-time PCR primers[a]

Target	Orientation[b]	Primer[a] sequence (5′-3′)
MIP-1α (SICA3)	F	TTGTGATTGTTTGCTCTGAGAGTTC
	R	CGGTCGTCACCAGACACACT
MIP-1β (SICA4)	F	CCCTGGCCTTTCCTTTCAGT
	R	AGCTTCCTCGCGGTGTAAGA
GRO-β (GRO2)	F	CTGCCCTTACAGGAACAGAAGAG
	R	CAAACACATTAGGCGCAATCC
IL-8	F	AAGGAACCATCTCACTGTGTGTAAAC
	R	ATCAGGAAGGCTGCCAAGAG
GAPDH	F	CAACGGATTTGGTCGTATTGG
	R	GGCAACAATATCCACTTTACCAGAGT

[a] Primers were designed with Primer Express software as described in Materials and Methods.
[b] F, forward; R; reverse.

Macroarrays. Atlas human cytokine/receptor cDNA expression arrays (Clontech, Palo Alto, Calif.), containing 268 immobilized human cDNAs, housekeeping controls, and negative controls in duplicate dots on nylon membranes, were used to detect cytokine and chemokine genes that are regulated by Stx1 and/or LPS. We previously showed that LPS treatment of THP-1 cells rapidly induced TNF-α and IL-1β transcripts (within 2 h), whereas the induction of cytokine transcripts required longer (4 to 8 h) exposures to Stx1 (12). Therefore, approximately 1.0×10^7 differentiated THP-1 cells plated in 100-mm-diameter cell culture plates were treated with Stx1, LPS, or Stx1 plus LPS for 2 or 6 h. Total RNAs were isolated, treated with DNase per the manufacturer's instructions, and stored at −70°C until use. In accordance with the manufacturer's protocol, the Atlas arrays were prehybridized at 68°C for 1 h with continuous agitation in ExpressHyb prehybridization solution containing 100 μg of sheared salmon testis DNA/ml (previously boiled for 5 min and chilled on ice prior to addition to the prehybridization solution). During the prehybridization step, 2 to 5 μg of total RNA was converted to ^{32}P-labeled cDNA by use of an Atlas Pure total RNA labeling system (Amersham Pharmacia Biotech Inc., Piscataway, N.J.). Unincorporated ^{32}P-labeled nucleotides were removed by column chromatography using spin columns provided with the Atlas Pure total RNA labeling system (Clontech). C_0t-1 DNA was added to the labeled probe to reduce background hybridization to repetitive DNA sequences prior to the addition of the probe to the hybridization solution. The probe was allowed to hybridize overnight at 68°C with continuous agitation. Blots were then washed three times with 100 ml of prewarmed wash solution I (2× SSC [1× SSC is 0.15 M NaCl plus 0.015 M sodium citrate], 1% sodium dodecyl sulfate [SDS]) for 30 min at 68°C, followed by one wash with 100 ml of prewarmed wash solution II (0.1× SSC, 0.5% SDS) at 68°C for 30 min. A final 5-min wash was performed with 100 ml of wash solution III (2× SSC) at room temperature. The Atlas arrays were then removed, wrapped in plastic, and exposed to X-ray film at −70°C with an intensifying screen. Screens were scanned by use of a PhosphorImager (Molecular Dynamics, Sunnyvale, Calif.) to visualize up- and down-regulated genes. The data were quantitated with ImageQuant software (Molecular Dynamics). The experiments were performed in duplicate, with glyceraldehyde-3-phosphate dehydrogenase (GAPDH) included for normalization. The complete gene list for the Atlas human cytokine/receptor cDNA expression array (7744–1) may be viewed at www.bdbiosciences.com/clontech/atlas/genelists/index.shtml.

Real-time PCR. Total RNAs were isolated by use of an RNeasy mini kit (Qiagen, Valencia, Calif.) with an RNase-free DNase (Qiagen) treatment for 30 min. Per the manufacturer's instructions, RNAs were reverse transcribed to cDNAs by the use of TaqMan reverse transcription reagents, and real-time PCRs were performed on the resulting cDNAs by the use of SYBR Green I double-stranded DNA binding dye (Applied Biosystems, Foster City, Calif.). Real-time primers specific for macrophage inflammatory protein 1α (MIP-1α; also called SICA3), MIP-1β (SICA4), growth-related oncogene β (GRO-β; also called GRO-2), IL-8, and GAPDH were designed with Primer Express software (Applied Biosystems) and are listed in Table 1. The real-time PCRs were carried out with a 100 nM concentration (each) of forward and reverse primers in a total volume of 25 μl. In order to control for the presence of contaminating DNA in the real-time reactions, we included reverse transcriptase-negative reactions. Template-negative controls were also run in order to test for DNA-contaminated

primers. Real-time reactions were run and analyzed by use of an ABI PRISM 7500 sequence detection system (Applied Biosystems). Dissociation curves for PCR samples were made by an additional denaturation step at 95°C for 15 s, annealing at 60°C for 20 s, and a slow increase in temperature back to 95°C with a ramp time of 19 min 59 s to guarantee amplification of the correct genes. The amount of induction of mRNA was determined from threshold cycle values normalized for GAPDH expression and then normalized to the value derived from cells at time zero prior to the medium change or treatment.

Northern blot analysis. To determine IL-8 mRNA kinetics and decay rates, we treated differentiated THP-1 cells with stimulants in the presence or absence of the transcriptional inhibitor actinomycin D (ActD; Sigma) according to the protocol of Harrold et al. (13). Based on the IL-8 mRNA kinetic data from this study, 5.0 μg of ActD/ml was added to the cells 1 h after treatment with LPS or Stx1 plus LPS or 6 h after Stx1 treatment. Two 1.0-ml aliquots of each cell supernatant were collected and stored at −20°C for use in enzyme-linked immunosorbent assays (ELISAs) (see below). Total RNAs were extracted from cells by the TRIzol reagent (Invitrogen) protocol for cell monolayers. After extraction, total RNA samples (up to 15 μg) were electrophoresed in 1.0% agarose-formaldehyde gels at 50 V for 1.5 h and then transferred to positively charged nylon membranes by use of a Turboblotter apparatus (Schleicher & Schuell, Keene, N.H.) for at least 3 h. Transferred RNAs were cross-linked to membranes by use of a UV cross-linker (Bio-Rad, Hercules, Calif.). The membranes were washed in 2× SSC–0.5% SDS for 30 to 60 min and then prehybridized at 42°C for at least 3 h in a 10-ml hybridization solution containing 100 μg of salmon testis DNA/ml, 2× SSC, 50% formamide (Sigma), 10% SDS, and 5× Denhardt's solution (Invitrogen) in diethyl pyrocarbonate-treated water. A human IL-8 cDNA probe was a kind gift from Cheleste Thorpe, Division of Geographic Medicine and Infectious Diseases, Department of Medicine, Tufts—New England Medical Center, Boston, Mass. Prior to prehybridization, IL-8 plasmid DNA was digested with EcoRI (New England Biolabs, Beverly, Mass.) to yield a 500-bp fragment containing 365 bp of the IL-8 gene in addition to sequences derived from a portion of the poly(A)$^+$ tail. Restriction fragments were visualized after electrophoresis of the digests in 1.2% agarose gels containing ethidium bromide. The 500-bp fragment was excised and purified by use of a QIAquick gel extraction kit (Qiagen). During the last hour of prehybridization, the IL-8 cDNA fragment was resuspended in 10 mM Tris–1.0 mM EDTA (TE), pH 8, to a total volume of 45 μl for use in [α-^{32}P]dCTP random primer labeling reactions performed with a Rediprime II kit (Amersham Pharmacia Biotech Inc.). A 316-bp human GAPDH DNA probe (Ambion Inc., Austin, Tex.) was randomly labeled by use of a Rediprime II kit to detect GAPDH mRNA, which served as an mRNA stability control as well as a loading control. After labeling, unincorporated [α-^{32}P]dCTP was removed by the use of TE-Midi-Select D G-50 Sephadex columns (Shelton Scientific, Shelton, Conn.). The labeled probes were ready to use after boiling for 5 min. ^{32}P-labeled probes were added to the hybridization solution overnight at 42°C. After hybridization, the blots were rinsed with 2× SSC, washed twice with 2× SSC–1.0% SDS for 15 min at room temperature, and then washed once with 0.1× SSC–1.0% SDS for 30 min at 60°C. The blots were dried briefly prior to exposure to a PhosphorImager screen and were analyzed by use of a PhosphorImager (Molecular Dynamics). The membranes were stripped by boiling in 0.1× SSC–0.1% SDS twice for 15 min and then sequentially reprobed with the GAPDH probe at 42°C. Quantitation of the pixel intensities of the RNA bands was done with ImageQuant software (Molecular Dynamics). All of the RNA data were normalized by dividing the IL-8 band intensities by the corresponding GAPDH band intensities at each time point. Kinetic data were then expressed as percentages of IL-8 mRNA above the basal level, determined as follows: [(intensity of stimulated cells − intensity of unstimulated cells)/(intensity of unstimulated cells)] × 100.

mRNA decay data were expressed as percentages of IL-8 mRNA remaining, determined as follows: (intensity of cells stimulated with ActD when $t = n$/intensity of cells stimulated with ActD when $t = 0$) × 100, where n equals the time of ActD exposure, so that when $n = 0$, the percentage of IL-8 mRNA remaining equals 100.

Chemokine ELISAs. Quantitation of secreted IL-8, MIP-1α, and MIP-1β protein concentrations was performed by the use of corresponding Quantikine colorimetric sandwich ELISA assay kits (R&D Systems, Minneapolis, Minn.). GRO-β protein concentrations were determined by use of a TiterZyme EIA human GRO-β enzyme immunometric assay kit from Assay Designs, Inc. (Ann Arbor, Mich.). Cellular debris was removed from the supernatants of treated cells by centrifugation. Dilutions of Stx1, LPS, and Stx1-plus-LPS samples were made when necessary, and kit-specified volumes of each sample were added in triplicate to the ELISA plate wells. The manufacturer's protocol was followed, and A_{450} and A_{570} were measured by a microtiter plate reader (MR5000; Dynatech Laboratories, Chantilly, Va.). Chemokine protein concentrations were calculated based on standard curves. The assay sensitivities were 4 pg/ml (IL-8), 10 pg/ml (MIP-1β), <10 pg/ml (MIP-1α), and 20.5 pg/ml (GRO-β).

Statistics. Statistics for experiments were performed with the SAS statistics program (SAS Institute, Cary, N.C.) or Excel (Microsoft Corporation, Redmond, Wash.). Real-time PCR inductions and IL-8 mRNA kinetics were analyzed by two-way analyses of variance (ANOVAs), with the Duncan multiple range test used for posthoc comparisons. IL-8 mRNA levels in decay experiments and IL-8, MIP-1α, MIP-1β, and GRO-β protein kinetics were analyzed by one-way ANOVAs, with the Duncan multiple range test used for posthoc analysis. For mRNA half-lives, the calculated half-lives were analyzed by Student's t test in Excel to compare IL-8 mRNA half-lives in LPS- and Stx1-treated cells. P values of ≤0.05 were considered significant for all analyses. All data are presented as means and standard errors of the means for a compilation of at least three independent experiments.

RESULTS

Macroarray analysis of cytokine and chemokine gene expression in THP-1 cells treated with Stx1 and/or LPS. Cytokine gene expression analysis was performed with differentiated THP-1 cells after incubation with Stx1, LPS, or Stx1 plus LPS for 2 or 6 h. Total RNAs isolated from treated and untreated cells were converted into ^{32}P-labeled cDNA probes and hybridized to identical arrays overnight (Fig. 1). Hybridization intensities were determined by use of a phosphorimager and were normalized to the internal control GAPDH. The induction level of genes in treated cells were calculated based on the hybridization intensities in untreated cells. Genes that were induced ≥2.0-fold were considered significantly up-regulated and those that were reduced ≤−1.0-fold were considered down-regulated. The changes in the expression of cytokine and chemokine transcripts after the treatment of differentiated THP-1 cells with Stx1 and/or LPS are summarized in Table 2. Only six genes were consistently up-regulated at least twofold by all treatments. These genes encoded MIP-1α (SICA3 or CCL3), MIP-1β (SICA4 or CCL4), TNF-α, IL-1β, IL-8, and GRO-β (GRO-2 or CXCL2). The only exception was IL-1β and IL-8 expression after Stx1 treatment for 2 h, for which the induction was <2.0-fold. Four of the six up-regulated genes encode CC or CXC chemokines, which primarily attract monocytes or neutrophils, respectively, to sites of infection. As previously noted for TNF-α and IL-1β expression (12), LPS and Stx1-plus-LPS treatments induced higher levels of chemokine gene expression than treatment with Stx1 alone.

Real-time PCR confirmation of chemokine mRNA expression in THP-1 cells. THP-1 cells were examined by quantitative real-time PCR to verify the expression of MIP-1α, MIP-1β, GRO-β, and IL-8 transcripts above that of untreated controls after treatment with Stx1, LPS, or both for 2 or 6 h (Fig. 2). At 2 h, treatment with LPS or Stx1 plus LPS resulted in a significant induction ($P \leq 0.05$) of MIP-1α and MIP-1β mRNAs compared to untreated controls, while GRO-β and IL-8 mRNA expression induction was only significant ($P \leq 0.05$) after treatment with Stx1 plus LPS (Fig. 2a). After 6 h, a significant induction ($P \leq 0.05$) of MIP-1α, MIP-1β, and GRO-β mRNAs occurred only when cells were treated with Stx1 plus LPS (Fig. 2a). IL-8 mRNA induction, however, was significantly elevated ($P \leq 0.05$) above untreated control levels after treatment with LPS or Stx1 plus LPS (Fig. 2a). Furthermore, from 2 to 6 h there was a significant increase ($P \leq 0.05$) in IL-8 mRNA levels for both LPS and Stx1-plus-LPS treat-

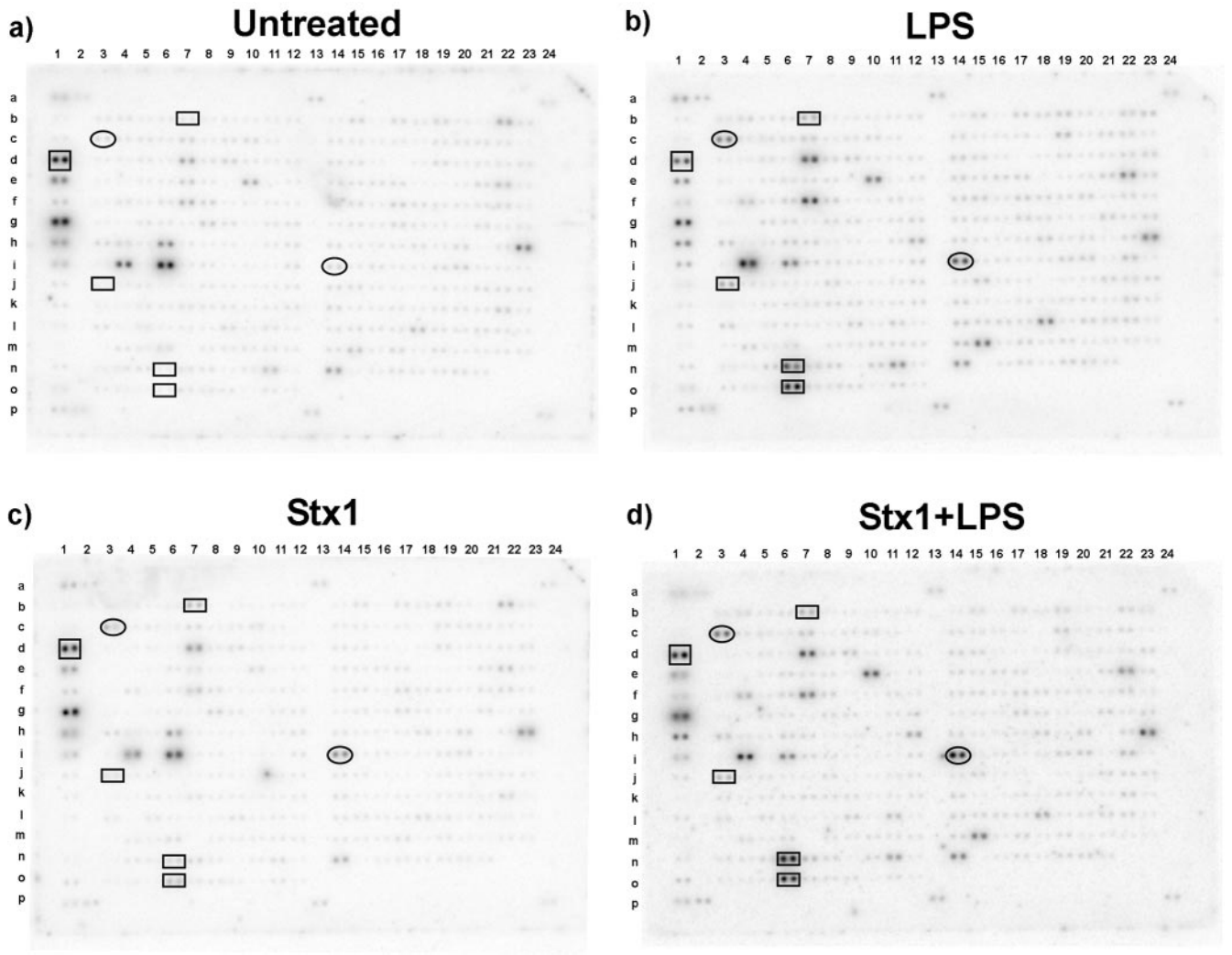

FIG. 1. Differential gene expression by THP-1 cells after treatment with Stx1, LPS, or Stx1 plus LPS, as measured by cDNA macroarrays. Differentiated THP-1 cells were left untreated, treated with 200 ng of LPS/ml, treated with 400 ng of Stx1/ml, or treated with Stx1 plus LPS for 6 h. Total RNAs were isolated and converted into ^{32}P-labeled cDNA probes by the use of reverse transcriptase. The probes were hybridized to membranes containing cDNAs derived from 268 cytokine and chemokine genes spotted in duplicate. Hybridization was detected by use of a phosphorimager. Paired spots within squares correspond to the GAPDH internal control (position 1d on the membranes). Pairs of spots identified by circles correspond to IL-1β (position 3c) and TNF-α (position 14i). Pairs of spots identified by rectangles correspond to IL-8 (position 3j), MIP-1α (position 6n), MIP-1β (position 6o), and GRO-β (position 7b).

ments (Fig. 2a). While MIP-1α and MIP-1β transcripts appeared to decrease from 2 to 6 h, these differences were not significant. In the case of GRO-β, the trend was similar to that of IL-8 in that transcript levels appeared to increase from 2 to 6 h, but this difference was also not significant. Interestingly, the Stx1-plus-LPS treatment induced significantly higher levels of IL-8 mRNA than LPS alone at 6 h ($P \leq 0.05$). Treatment with Stx1 alone appeared to induce chemokine levels above those of untreated controls at 2 or 6 h (Fig. 2b), but two-way ANOVAs did not reveal significant differences compared to untreated controls.

IL-8 mRNA kinetics in THP-1 cells treated with Stx1 and/or LPS. Previous reports showed that Stx1 treatment of human intestinal epithelial cell lines resulted in the expression of IL-8 (45, 53). However, our real-time PCR studies suggested that Stx1 did not significantly activate IL-8 gene expression in macrophage-like THP-1 cells within 6 h of toxin treatment. Therefore, we used Northern blot analyses to more extensively characterize the IL-8 transcriptional response to Stx1 and/or LPS. When THP-1 cells were treated with LPS or Stx1 plus LPS (Fig. 3a), IL-8 transcript induction occurred rapidly and with indistinguishable kinetics until 16 and 24 h posttreatment, when Stx1-plus-LPS-induced IL-8 transcript levels were significantly higher than LPS-induced transcript levels ($P = 0.0014$ at 16 h and $P = 0.0005$ at 24 h). Due to the rapid induction of apoptosis in Stx1-plus-LPS-treated THP-1 cells (L. M. Harrison and V. L. Tesh, submitted for publication), we were unable to extract adequate RNA for Northern blots past the 24-h time point. The treatment of cells with Stx1 alone resulted in a relatively slow induction of IL-8 transcripts, with significantly elevated levels first reached at 12 h posttreatment and peaking at 36 h (Fig. 3b). In terms of maximal IL-8 transcript levels

TABLE 2. Induction of up- and down-regulated genes in Stx1- and/or LPS-treated THP-1 cells

Encoded protein	Functional category	GenBank accession	Fold induction[a]					
			Stx1		LPS		Stx1 + LPS	
			2 h	6 h	2 h	6 h	2 h	6 h
SICA3	Chemokine	M23452	2.2	3.9	27.5	33.8	48.2	91.1
SICA4	Chemokine	J04130	3.4	6.8	8.5	81.6	155.1	55.5
TNF-α	Cytokine	X01394	7.9	6.6	25.1	31.8	40.1	37.7
IL-1β	Cytokine	K02770	1.6	3.7	11	22	34.9	28.9
IL-8	Chemokine	Y00787	1.6	2.4	6.4	12.2	14.8	11.7
GRO-2	Chemokine	X53779	2.5	4.7	9.2	9.1	11.9	11.1
SICA2	Chemokine	M24545	1.7	1.4	NC	7.9	NC	8.9
SICA5	Chemokine	M21121	NC	NC	3.2	5.4	3.4	8.6
ET-2	Chemokine	M65199	2.7	NC	NC	NC	2.7	10.9
BMP4	Chemokine	D30751	NC	−3.0	1.6	1.9	3.2	−1.6
SCBPA8	Chemokine	X06234	2.4	−1.2	NC	2.0	NC	NC
CRHR1	Chemokine receptor	X72304	NC	NC	NC	NC	1.8	−2.4
FKTR3	Chemokine	U04806	NC	NC	NC	NC	1.9	−2.5

[a] NC, no change; fold induction values of $<+2.0$ to >-1.0.

above basal values, LPS induced approximately 5 times more and Stx1 plus LPS induced approximately 10 times more IL-8 mRNA than treatment with Stx1 alone.

Stx1 and Stx1 plus LPS induce IL-8 transcripts with increased stabilities compared to IL-8 transcripts induced by LPS. We previously reported that increased TNF-α and IL-1β mRNA stabilities may be involved in the maintenance of elevated TNF-α and IL-1β transcript levels after the treatment of THP-1 cells with Stx1 in the presence or absence of LPS (12). An increased IL-8 mRNA stability associated with Stx1 treatment of intestinal epithelial cells has also been reported (46). To determine whether Stx1 affects IL-8 transcript stability, we treated THP-1 cells with Stx1 for 6 h and with LPS or Stx1 plus LPS for 1 h and then added the transcriptional inhibitor actinomycin D to measure mRNA decay rates by Northern blot analyses. LPS-induced transcripts were labile, with a calculated half-life of 1.2 h (Fig. 4a). Stx1- and Stx1-plus-LPS-induced IL-8 transcripts decayed more slowly (Fig. 4b). The calculated half-life for Stx1-induced IL-8 mRNA was 4.1 h, while the half-life for Stx1-plus-LPS-induced IL-8 mRNA was longer than the time course of the experiment (≥5 h). A statistical analysis revealed that IL-8 mRNA from cells treated with Stx1 had a significantly longer half-life than IL-8 mRNA from cells treated with LPS ($P = 0.02$). Although we did not determine a half-life for IL-8 transcripts induced by Stx1 plus LPS, a statistical analysis of IL-8 mRNA levels indicated that Stx1-induced IL-8 transcript levels were significantly lower than the Stx1-plus-LPS-induced levels over time, and thus the half-life of Stx1-plus-LPS-induced IL-8 mRNA was also significantly longer than the half-life of LPS-induced mRNA.

Treatment of THP-1 cells with Stx1, LPS, and Stx1 plus LPS results in IL-8 protein production. Fig. 5 shows the induction of IL-8 protein over time for THP-1 cells treated with LPS, Stx1, and Stx1 plus LPS. In general, IL-8 protein production correlated with IL-8 mRNA expression. For cells treated with LPS (Fig. 5a), IL-8 expression was significantly elevated ($P \leq 0.05$) at 4 h posttreatment, with a peak concentration of 151.8 ng/ml reached at 72 h. IL-8 protein levels from Stx1-treated cells (Fig. 5b) were not elevated above control levels until 8 h after treatment, with significant elevations occurring at 24 h ($P \leq 0.05$). Peak IL-8 protein expression by Stx1-treated cells was approximately 15-fold less than that by LPS-treated cells. This observation is consistent with previous reports showing that Stx1 is a less potent inducer of TNF-α and IL-1β than is LPS (12, 35). For cells treated with Stx1 plus LPS (Fig. 5c), significantly elevated IL-8 expression was reached after 3 h. However, the treatment of THP-1 cells with both stimulants resulted in less IL-8 protein than that predicted based on the levels of IL-8 mRNA induced by Stx1 plus LPS. The "spike" of IL-8 mRNA we noted after 16 h of Stx1-plus-LPS exposure did not manifest as markedly increased IL-8 protein synthesis.

MIP-1α, MIP-1β, and GRO-β protein expression in THP-1 cells treated with Stx1, LPS, and Stx1 plus LPS. We examined the patterns of expression of the monocyte chemoattractants MIP-1α and MIP-1β and the neutrophil chemoattractant GRO-β after 24-h treatments of THP-1 cells with Stx1, LPS, and Stx1 plus LPS. Within 4 h, relatively high levels of MIP-1α (Fig. 6a) and MIP-1β (Fig. 6b) were expressed by cells that were treated with all of the stimulants, reaching concentrations of 20 to 40 ng/ml. LPS was the most significant ($P \leq 0.05$) stimulant of MIP-1α and MIP-1β expression, while Stx1 was the least robust inducer of these chemokines. MIP-1α and MIP-1β levels induced by LPS or Stx1 plus LPS roughly doubled over the next 8 h of stimulation and then remained constant for the remainder of the experiment. The levels of MIP-1α and MIP-1β induced by Stx1 did not appear to increase significantly beyond the 4-h time point. GRO-β expression (Fig. 6c) was slower and continued to rise for all treatments throughout the course of the experiments. As was the case for the IL-8 protein, the treatment of cells with Stx1 plus LPS resulted in the synthesis or release of the MIP-1α, MIP-1β, and GRO-β proteins at intermediate levels between those induced by treatments with Stx1 alone and LPS alone.

DISCUSSION

Given the property of TNF-α and IL-1β to modulate toxin receptor expression on vascular endothelial cells, our earlier studies focused on the mechanisms by which Stxs signal proinflammatory cytokine expression by macrophages (7, 12, 35).

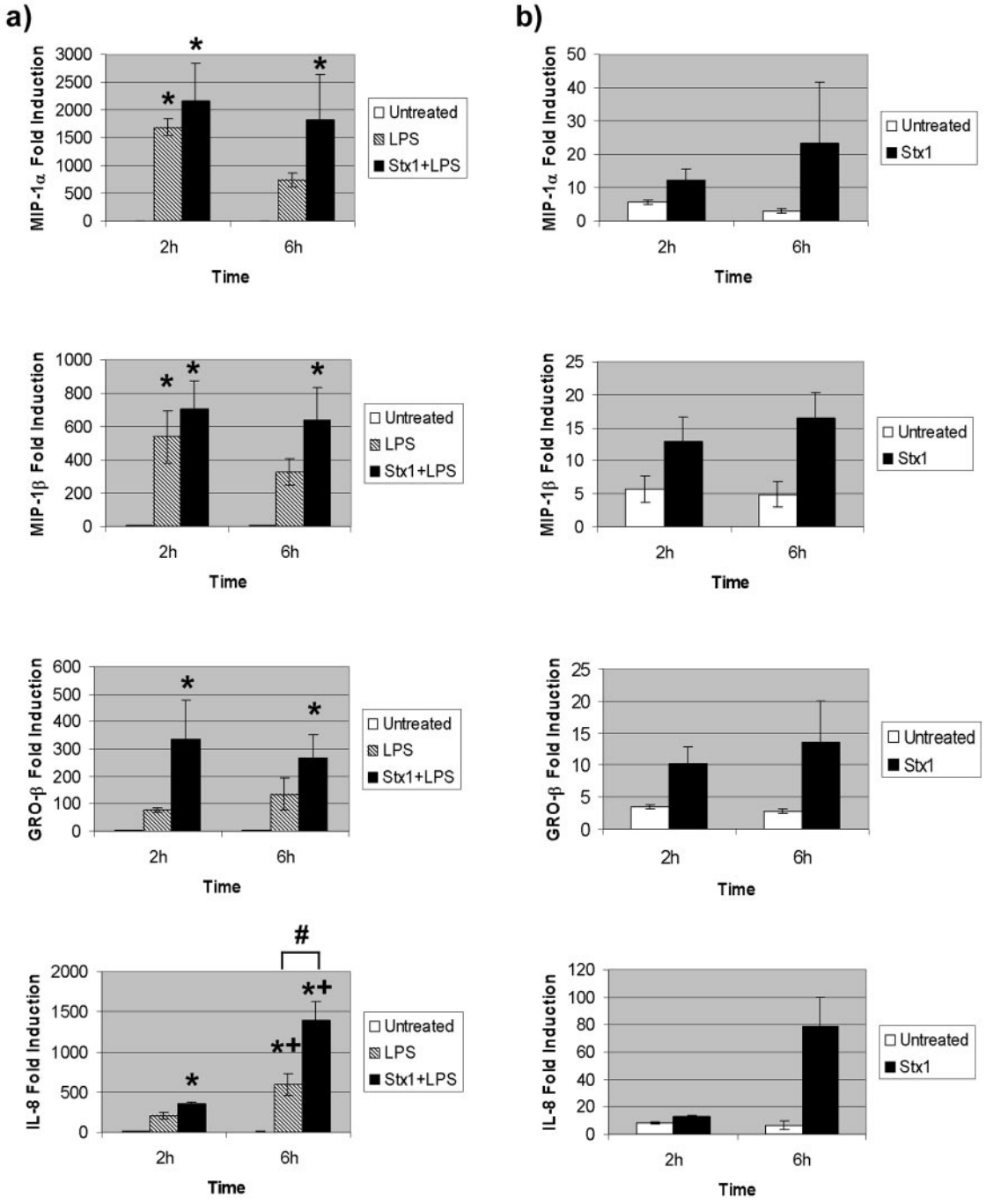

FIG. 2. Real-time PCR verification of chemokine expression in Stx1- and/or LPS-treated THP-1 cells. Differentiated THP-1 cells (5×10^6 cells/ml) were incubated with medium alone (open bars), 200 ng of LPS/ml (hatched bars), or Stx1 plus LPS (closed bars) (a) or with medium alone (open bars) or 400 ng of Stx1/ml (closed bars) (b) for 2 or 6 h. Threshold cycle values were normalized for GAPDH expression, and the levels of induction of MIP-1α, MIP-1β, GRO-β, and IL-8 expression were calculated relative to the 0-h untreated control. Data are expressed as means ± standard errors of the means (error bars) for three or four independent experiments. An asterisk (*) denotes a significant difference ($P \leq 0.05$) between treatments at each time point for each cytokine. A plus sign (+) denotes a significant difference ($P \leq 0.05$) between the 2- and 6-h cytokine induction levels within each treatment. A number sign (#) denotes a significant difference ($P \leq 0.05$) in cytokine induction between treatments within a time point.

For this study, we used commercially available macroarrays spotted with cytokine and chemokine cDNAs to obtain a more global view of the macrophage transcriptional response to Stx1 and/or LPS. We showed that genes encoding the following six proteins were consistently up-regulated in response to the bacterial products: the proinflammatory cytokines TNF-α and IL-1β, the CC chemokines MIP-1α and MIP-1β, and the CXC chemokines IL-8 and GRO-β. For four of the six genes, the

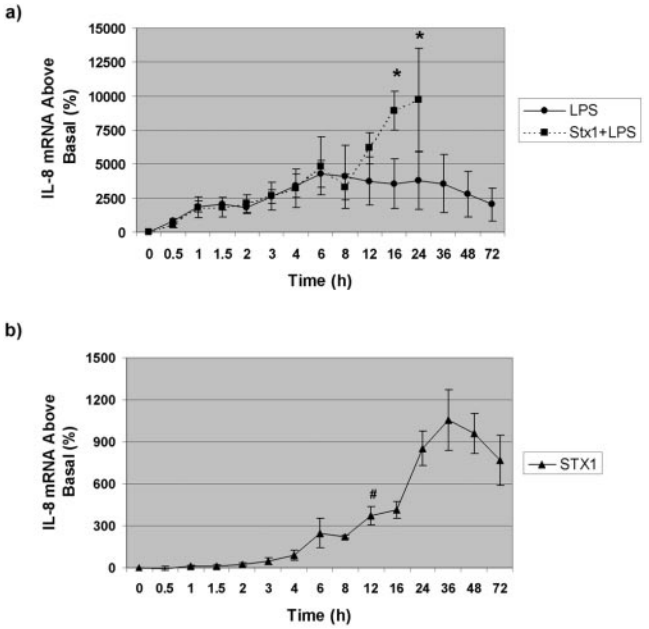

FIG. 3. Comparison of IL-8 mRNA expression in THP-1 cells treated with Stx1, LPS, and Stx1 plus LPS. Differentiated THP-1 cells (5×10^6 cells/ml) were treated with 400 ng of Stx1/ml, 200 ng of LPS/ml, or both for 0 to 72 h. Total RNAs (5 to 15 μg) were subjected to Northern blot analysis with ^{32}P-labeled IL-8 and GAPDH cDNA probes. Hybridization was detected and quantitated by use of a phosphorimager and was expressed as a percentage of IL-8 mRNA above basal (unstimulated) expression. The data are expressed as means ± standard errors of the means (error bars) for at least three independent experiments with LPS- and Stx1-plus-LPS-treated THP-1 cells (a) and Stx1-treated THP-1 cells (b). An asterisk (*) denotes a significant difference ($P \leq 0.05$) between the LPS and Stx1-plus-LPS treatments. A number sign (#) denotes the first point of significant induction for Stx1-induced IL-8 mRNA; data for all time points of ≥12 h were significantly different from that at the zero time point.

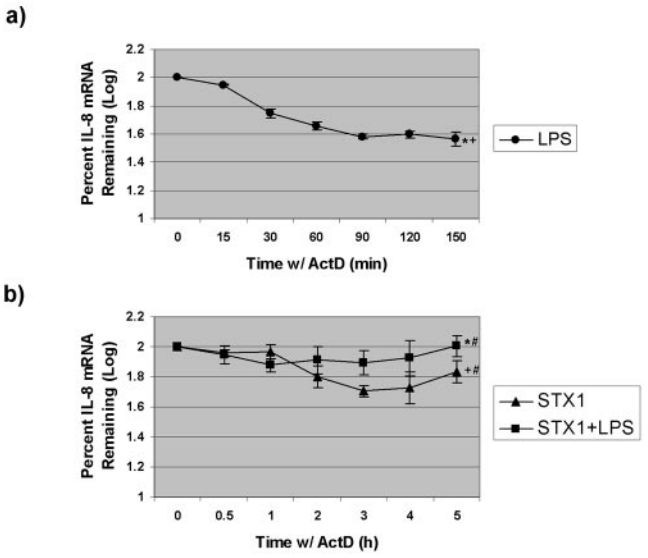

FIG. 4. Effects of Stx1 and/or LPS on IL-8 mRNA stability in THP-1 cells. Differentiated THP-1 cells (5×10^6 cells/ml) were treated with LPS (200 ng/ml) for 1 h (a) or with Stx1 (400 ng/ml) for 6 h or Stx1 plus LPS for 1 h (b). Actinomycin D (ActD) was then added to each plate at a final concentration of 5.0 μg/ml. Total RNAs were isolated at each of the indicated time points after ActD addition. Northern blot analysis was performed, and IL-8 mRNA was detected and quantitated by use of a phosphorimager. The data are expressed as means of the percentages of IL-8 mRNA remaining (log) ± standard errors of the means (error bars) for at least three independent experiments. Treatments with the same symbol were significantly different ($P \leq 0.05$) from each other.

levels of transcripts induced by treatment with Stx1 plus LPS were higher than those of transcripts induced by either treatment alone at the 2- and 6-h time points. The exceptions were the chemokines IL-8 and MIP-1β, for which treatment with LPS alone for 6 h induced larger increases than treatment with Stx1 plus LPS. Other genes showed more complex patterns of induction. Monocyte chemotactic protein 1 (SICA2 or CCL2) was only up-regulated after 6-h treatments with LPS or Stx1 plus LPS. RANTES (SICA5 or CCL5) was induced by LPS, and its expression was increased by Stx1 plus LPS. Endothelin-2 (ET2) was induced early (2 h) by Stx1 and Stx1 plus LPS, and ET2 mRNA levels were increased by treatment with Stx1 plus LPS at 6 h. Bone morphogenetic protein 4 (BMP4) was induced early by Stx1 plus LPS, but its levels were down-regulated by a longer exposure to Stx1 or Stx1 plus LPS. Corticotropin-releasing hormone receptor 1 (CRHR1) and fms-related tyrosine kinase 3 ligand (FKTR3) were modestly down-regulated by exposure to Stx1 plus LPS. S100 calcium-binding protein A8 (SCBPA8) was the only transcript that was up-regulated early (2 h) in response to treatment with Stx1 alone.

We used chemokine-specific forward and reverse primers to conduct real-time PCRs to verify the chemokine expression patterns of Stx1-, LPS-, and Stx1-plus-LPS-treated THP-1 cells. In accordance with the macroarray data, Stx1 treatment alone induced modest levels of chemokine transcripts at 2 and 6 h. At 2 h, LPS induced significant levels of the CC chemokines MIP-1α and MIP-1β ($P \leq 0.05$) but did not induce significant levels of the CXC chemokines IL-8 and GRO-β. Six hours after LPS treatment, the levels of MIP-1α and MIP-1β transcripts were not significantly different from those in untreated cells, suggesting that transcriptional activation may be transient or that the mRNA transcripts are labile. LPS induced modest levels of GRO-β transcripts, while 6 h of LPS treatment produced a significant level ($P \leq 0.05$) of IL-8 mRNA expression. After both 2 and 6 h of Stx1-plus-LPS treatment, significant levels of all of the observed chemokines were expressed ($P \leq 0.05$).

We noted some discrepancies between the macroarray and real-time PCR results. For example, the macroarray data suggested that there was a slight decrease in IL-8 transcripts induced by Stx1 plus LPS between 2 and 6 h, yet the real-time PCR data showed an increase in IL-8 mRNA induced by Stx1 plus LPS between the 2- and 6-h time points. To examine in more detail the kinetics of IL-8 mRNA expression by THP-1 cells treated with Stx1 and/or LPS, we utilized Northern blot analysis. The treatment of cells with Stx1 alone resulted in a slow induction of IL-8 mRNA expression, with significant transcript elevation noted 12 h after toxin treatment. In contrast, LPS and Stx1-plus-LPS treatments induced IL-8 transcripts with almost identical rapid kinetics until 16 to 24 h posttreatment, when the levels of IL-8 mRNA expressed by Stx1-plus-

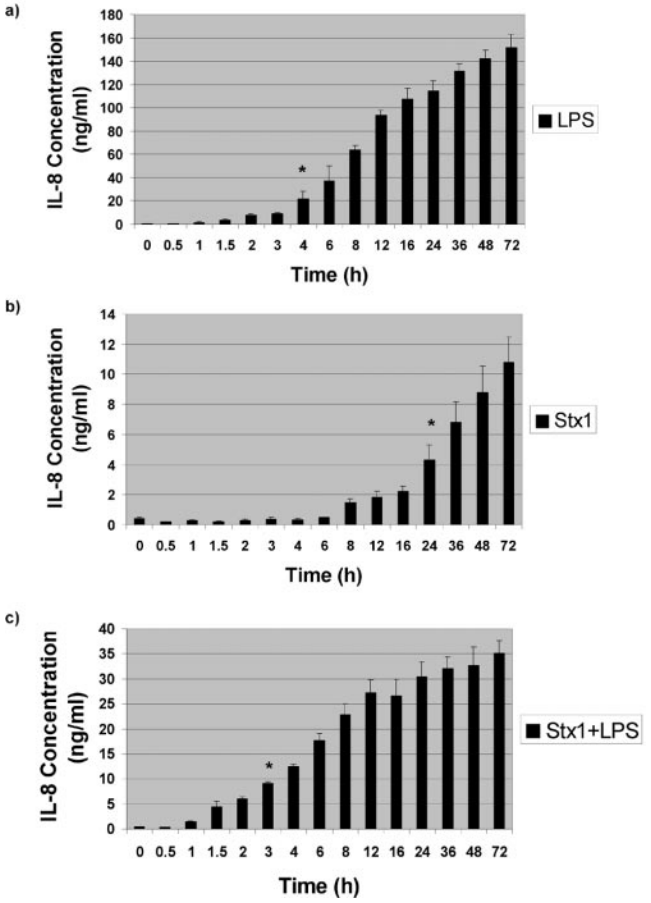

FIG. 5. IL-8 protein production by THP-1 cells treated with Stx1, LPS, and Stx1 plus LPS. Cell-free supernatants from cells treated with LPS (a), Stx1 (b), or Stx1 plus LPS (c) were collected and analyzed by a human IL-8-specific ELISA. The data shown are means ± standard errors of the means (error bars) for at least three independent experiments. Asterisks (*) denote the first significant expression difference ($P \leq 0.05$) between untreated and treated cells; data for all time points beyond this point were significantly different from the zero time point.

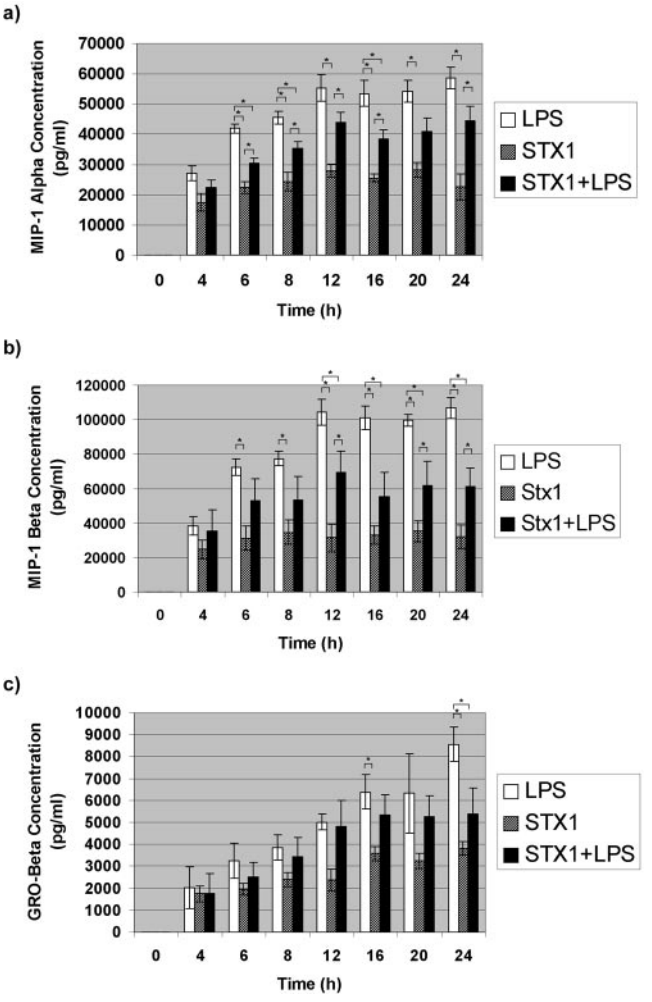

FIG. 6. MIP-1α, MIP-1β, and GRO-β protein production by THP-1 cells treated with Stx1, LPS, or Stx1 plus LPS. Cell-free supernatants from LPS-, Stx1-, and Stx1-plus-LPS-treated cells were collected and analyzed by ELISAs specific for human MIP-1α (a), MIP-1β (b), and GRO-β (c). The data shown are means ± standard errors of the means (error bars) for at least three independent experiments. Significant differences between treatments are indicated by asterisks (*).

LPS-treated cells were significantly elevated compared to those in cells treated with LPS alone. We have shown that the treatment of macrophage-like THP-1 cells with Stx1 plus LPS results in programmed cell death (Harrison and Tesh, submitted), and at later time points we were unable to extract adequate amounts of RNA to perform Northern blots. These data suggest that coincident with apoptotic signaling induced by Stx1 plus LPS, the IL-8 gene may become transcriptionally active.

Thorpe et al. (46) reported that Stx1 treatment of a human intestinal epithelial cell line stabilized IL-8 mRNA transcripts. To determine whether changes in mRNA stability were involved in the higher levels of IL-8 transcripts noted at later time points for Stx1- and/or LPS-treated THP-1 cells, we used the transcriptional inhibitor actinomycin D to measure transcript decay rates. LPS-induced IL-8 transcripts had a significantly shorter half-life (1.2 h; $P \leq 0.05$) than Stx1- and Stx1-plus-LPS-induced IL-8 transcripts (4.1 and >5 h, respectively). Measurements of soluble IL-8 production suggested that IL-8 transcripts and protein induced by Stx1 or LPS treatments were correlated in that Stx1 induced a delayed expression of IL-8 mRNA and protein, while LPS induced earlier, more robust IL-8 mRNA and protein responses. This direct correlation between transcription and translation did not manifest in Stx1-plus-LPS-treated cells. Given the spike of IL-8 mRNA expression and the increased stability of IL-8 mRNA induced by Stx1 plus LPS treatment, we predicted that soluble IL-8 protein levels induced by both stimulants would exceed that produced by cells treated with LPS alone. We found that the amount of IL-8 protein elicited by Stx1-plus-LPS treatment was fivefold less than that induced by LPS. This pattern of diminished protein expression in response to Stx1-plus-LPS treatment was also evident for MIP-1α, MIP-1β, and GRO-β expression. Thus, in contrast to our earlier studies, in which Stx1-plus-LPS treatment augmented the production of soluble TNF-α (35), Stx1 appears to down-modulate the macrophage chemokine response to LPS.

Before Stxs elicit proinflammatory cytokine expression, they must traverse the intestinal epithelial cell barrier, and several studies have shown that Stxs are transported in an apical-to-basolateral manner across polarized intestinal epithelial cell monolayers via energy-dependent transcytotic mechanisms (14, 30). Neutrophil infiltration of the colonic submucosa and fecal leukocytosis are characteristics of the colitis caused by Stx-producing bacteria (40). Stxs have been shown to directly induce the expression of the neutrophil chemoattractants IL-8 and GRO-α by intestinal epithelial cells in vitro (45, 46, 53). These data suggest that Stxs not only possess the capacity to breach the intestinal epithelium, but may also contribute to the processes of neutrophil extravasation and migration into the lamina propria and transmigration across the epithelium. Hurley et al. (15) showed that the basolateral-to-apical migration of neutrophils across intestinal epithelial cell monolayers resulted in enhanced paracellular transport of Stxs across the monolayers. Thus, the localized production of IL-8 and other chemokines in response to Stxs may establish an amplification loop in which the gut is made markedly more permeable to Stxs and other bacterial constituents such as LPS.

It has proven difficult to detect circulating Stxs in the blood, and the precise means of systemic toxin transport remain to be fully characterized. Following translocation into the lamina propria or destruction of the colonic epithelium, Stxs may be in an environment that is rich in neutrophils and macrophages. The toxins may delay the onset of neutrophil apoptosis, thereby extending the life span of these short-lived cells (21). te Loo et al. (41) have reported that Stx1 binds to neutrophils in blood plasma via a relatively low-affinity interaction with a non-Gb_3 receptor. Furthermore, functional Stx1 can be transferred from neutrophils to endothelial cells in vitro. These findings raise the possibility that the elicitation of a neutrophil infiltrate in the lamina propria may provide cells to which Stxs "piggyback" for distribution to the microvasculature of target organs.

In addition to acting as chemoattractants for cells that increase intestinal permeability and serve to disseminate toxins, IL-8 and the GRO proteins are known to activate the phagocytic and respiratory burst activities of neutrophils and basophils (10, 52). All three GRO proteins are expressed by macrophages in response to LPS treatment, and the GRO-α protein is expressed by Stx1-treated intestinal epithelial cells (11, 46). We show here that Stx1 and LPS induce the expression of the GRO-β protein from THP-1 cells. By activating neutrophils, IL-8 and GRO-β production may contribute to the development of extraintestinal disease triggered by Stxs. Neutrophils isolated from HUS patients are more adherent to endothelial cell monolayers and mediate more destruction of underlying fibronectin substrates than neutrophils isolated from healthy controls (6). The levels of urinary IL-8 and monocyte chemoattractant protein 1 are frequently elevated in HUS patients and correlate with neutrophil and monocyte infiltration into the kidneys (16, 50). The levels of IL-8 in the plasma of HUS patients positively correlate with leukocytosis and plasma elastase levels, a marker of neutrophil activation (4). Finally, chemokines produced in response to Stxs may facilitate platelet activation and aggregation (9).

MIP-1α and MIP-1β are powerful monocyte chemoattractants that activate cells by increasing intracellular [Ca^{2+}] and releasing arachidonic acid (reviewed in reference 24). MIP-1α production by macrophages is increased following engagement with intercellular adhesion molecule 1 expressed on the surfaces of endothelial cells (23). Renal biopsies from patients with inflammatory glomerulonephritis revealed elevated MIP-1α and MIP-1β mRNA levels in glomerular leukocyte infiltrates (2). IL-1β-treated human astrocytes release MIP-1α proteins and human brain microvascular endothelial cells release MIP-1β in response to treatment with LPS, TNF-α, gamma interferon, or IL-1β (25, 38). Collectively, these data suggest that the localized production of MIP-1α and MIP-1β in the kidneys and brain in response to Stxs and/or LPS, particularly at sites of monocyte-endothelial cell adherence, may further exacerbate vascular damage.

ACKNOWLEDGMENTS

This work was supported by U.S. Public Health Service grant 2RO1 AI34530 from the National Institute of Allergy and Infectious Diseases.

The expert technical assistance of Christopher Thompson is gratefully acknowledged. We thank Cheleste Thorpe for the gift of IL-8 cDNA and Shannon Sedberry Allen, Wei-Jung Chen, and Rajesh Miranda for assistance with statistical analyses.

REFERENCES

1. **Auwerx, J.** 1991. The human leukemia cell line, THP-1: a multifaceted model for the study of monocyte-macrophage differentiation. Experientia **44:**22–31.
2. **Cockwell, P., A. J. Howie, D. Adu, and C. O. Savage.** 1998. In situ analysis of C-C chemokine mRNA in human glomerulonephritis. Kidney Int. **54:**827–836.
3. **Endo, Y., K. Tsurugi, T. Yutsudo, Y. Takeda, T. Ogasawara, and K. Igarashi.** 1988. Site of action of a Vero toxin (VT2) from *Escherichia coli* O157:H7 and Shiga toxin on eukaryotic ribosomes. RNA *N*-glycosidase activity of the toxins. Eur. J. Biochem. **171:**45–50.
4. **Fitzpatrick, M. M., V. Shah, R. S. Trompeter, M. J. Dillon, and T. M. Barratt.** 1992. Interleukin-8 and polymorphonuclear leucocyte activation in hemolytic uremic syndrome of childhood. Kidney Int. **42:**951–956.
5. **Fontaine, A., J. Arondel, and P. J. Sansonetti.** 1988. Role of Shiga toxin in the pathogenesis of bacillary dysentery, studied by using a Tox^- mutant of *Shigella dysenteriae* 1. Infect. Immun. **56:**3099–3109.
6. **Forsyth, K. D., A. C. Simpson, M. M. Fitzpatrick, T. M. Barratt, and R. J. Levinsky.** 1989. Neutrophil-mediated endothelial injury in haemolytic uraemic syndrome. Lancet **ii:**411–414.
7. **Foster, G. H., and V. L. Tesh.** 2002. Shiga toxin 1-induced activation of c-Jun NH_2-terminal kinase and p38 in the human monocytic cell line THP-1: possible involvement in the production of TNF-α. J. Leukoc. Biol. **71:**107–114.
8. **Fraser, M. E., M. M. Chernaia, Y. V. Kozlov, and M. N. G. James.** 1994. Crystal structure of the holotoxin from *Shigella dysenteriae* at 2.5 Å resolution. Nat. Struct. Biol. **1:**59–64.
9. **Gear, A. R., S. Suttitanamongkol, D. Viisoreanu, R. K. Polanowska-Grabowska, S. Raha, and D. Camerini.** 2001. Adenosine diphosphate strongly potentiates the ability of the chemokines MDC, TARC, and SDF-1 to stimulate platelet function. Blood **97:**937–945.
10. **Geiser, T., B. Dewald, M. U. Ehrengruber, I. Clark-Lewis, and M. Baggiolini.** 1993. The interleukin-8-related chemotactic cytokines GROα, GROβ, and GROγ activate human neutrophil and basophil leukocytes. J. Biol. Chem. **268:**15419–15424.
11. **Goodman, R. B., R. M. Strieter, C. W. Frevert, C. J. Cummings, P. Tekamp-Olson, S. L. Kunkel, A. Walz, and T. R. Martin.** 1998. Quantitative comparison of C-X-C chemokines produced by endotoxin-stimulated human alveolar macrophages. Am. J. Physiol. **275:**L87–L95.
12. **Harrison, L. M., W. C. E. van Haaften, and V. L. Tesh.** 2004. Regulation of proinflammatory cytokine expression by Shiga toxin 1 and/or lipopolysaccharides in the human monocytic cell line THP-1. Infect. Immun. **72:**2618–2627.
13. **Harrold, S., C. Genovese, B. Kobrin, S. L. Morrison, and C. Milcarek.** 1991. A comparison of apparent mRNA half-life using kinetic labeling techniques vs. decay following administration of transcriptional inhibitors. Anal. Biochem. **198:**19–29.
14. **Hurley, B. P., M. Jacewicz, C. M. Thorpe, L. L. Lincicome, A. J. King, G. T. Keusch, and D. W. K. Acheson.** 1999. Shiga toxins 1 and 2 translocate differently across polarized intestinal epithelial cells. Infect. Immun. **67:**6670–6677.
15. **Hurley, B. P., C. M. Thorpe, and D. W. K. Acheson.** 2001. Shiga toxin

translocation across intestinal epithelial cells is enhanced by neutrophil transmigration. Infect. Immun. **69:**6148–6155.
16. **Inward, C. D., A. J. Howie, M. M. Fitzpatrick, F. Rafaat, D. V. Milford, and C. M. Taylor.** 1997. Renal histopathology in fatal cases of diarrhea-associated haemolytic uraemic syndrome. Pediatr. Nephrol. **11:**556–559.
17. **Jacewicz, M., H. Clausen, E. Nudelman, A. Donohue-Rolfe, and G. T. Keusch.** 1986. Pathogenesis of *Shigella* diarrhea. XI. Isolation of a *Shigella* toxin-binding glycolipid from rabbit jejunum and HeLa cells and its identification as globotriaosylceramide. J. Exp. Med. **163:**1391–1404.
18. **Lindberg, A. A., J. E. Schultz, M. Westling, J. E. Brown, S. W. Rothman, K.-A. Karlsson, and N. Strömberg.** 1986. Identification of the receptor glycolipid for Shiga toxin produced by *Shigella dysenteriae* type 1, p. 439–446. *In* D. L. Lark (ed.), Protein carbohydrate interactions in biological systems. Academic Press, London, United Kingdom.
19. **Lingwood, C. A., A. A. Khine, and S. Arab.** 1998. Globotriaosyl ceramide (Gb_3) expression in human tumour cells: intracellular trafficking defines a new retrograde transport pathway from the cell surface to the nucleus, which correlates with sensitivity to verotoxin. Acta Biochim. Pol. **45:**351–359.
20. **Lingwood, C. A., H. Law, S. Richardson, M. Petric, J. L. Brunton, S. DeGrandis, and M. A. Karmali.** 1987. Glycolipid binding of purified and recombinant *Escherichia coli*-produced verotoxin *in vitro.* J. Biol. Chem. **262:** 8834–8839.
21. **Liu, J., T. Akahoshi, T. Sasahana, H. Kitasato, R. Namai, T. Sasaki, M. Inoue, and H. Kondo.** 1999. Inhibition of neutrophil apoptosis by verotoxin 2 derived from *Escherichia coli* O157:H7. Infect. Immun. **67:**6203–6205.
22. **Louise, C., and T. G. Obrig.** 1991. Shiga toxin-associated hemolytic uremic syndrome: combined cytotoxic effects of Shiga toxin, interleukin-1β, and tumor necrosis factor alpha on human vascular endothelial cells in vitro. Infect. Immun. **59:**4173–4179.
23. **Lukacs, N. W., R. M. Strieter, V. M. Elner, H. L. Evanoff, M. Burdick, and S. L. Kunkel.** 1994. Intercellular adhesion molecule-1 mediates the expression of monocyte-derived MIP-1α during monocyte-endothelial cell interactions. Blood **83:**1174–1178.
24. **Menten, P., A. Wuyts, and J. van Damme.** 2002. Macrophage inflammatory protein-1. Cytokine Growth Factor Rev. **13:**455–481.
25. **Miyamoto, Y., and S. U. Kim.** 1999. Cytokine-induced production of macrophage inflammatory protein-1α (MIP-1α) in cultured human astrocytes. J. Neurosci. Res. **55:**245–251.
26. **Moxley, R. A., and D. H. Francis.** 1998. Overview of animal models, p. 249–260. *In* J. B. Kaper and A. D. O'Brien (ed.), *Escherichia coli* O157:H7 and other Shiga toxin-producing *E. coli* strains. ASM Press, Washington, D.C.
27. **O'Brien, J. M., and E. Abraham.** 2004. Human models of endotoxemia and recombinant human activated protein C. Crit. Care Med. **32**(Suppl. 5)**:**S202–S208.
28. **Obrig, T. G., P. J. DelVecchio, J. E. Brown, T. P. Moran, B. M. Rowland, T. K. Judge, and S. W. Rothman.** 1988. Direct cytotoxic action of Shiga toxin on human vascular endothelial cells. Infect. Immun. **56:**2373–2378.
29. **Paton, J. C., and A. W. Paton.** 1998. Pathogenesis and diagnosis of Shiga toxin-producing *Escherichia coli* infections. Clin. Microbiol. Rev. **11:**450–479.
30. **Philpott, D. J., C. A. Ackerley, A. J. Killiaan, M. A. Karmali, M. H. Perdue, and P. M. Sherman.** 1997. Translocation of verotoxin-1 across T84 monolayers: mechanism of bacterial toxin penetration of epithelium. Am. J. Physiol. **273:**G1349–G1358.
31. **Proulx, F., E. G. Seidman, and D. Karpman.** 2001. Pathogenesis of Shiga toxin-associated hemolytic uremic syndrome. Pediatr. Res. **50:**163–171.
32. **Ramegowda, B., and V. L. Tesh.** 1996. Differentiation-associated toxin receptor modulation, cytokine production, and sensitivity to Shiga-like toxins in human monocytes and monocytic cell lines. Infect. Immun. **64:**1173–1180.
33. **Ramegowda, B., J. E. Samuel, and V. L. Tesh.** 1999. Interaction of Shiga toxins with human brain microvascular endothelial cells: cytokines as sensitizing agents. J. Infect. Dis. **180:**1205–1213.
34. **Ruggenenti, P., M. Noris, and G. Remuzzi.** 2001. Thrombotic microangiopathy, hemolytic uremic syndrome, and thrombotic thrombocytopenic purpura. Kidney Int. **60:**831–846.
35. **Sakiri, R., B. Ramegowda, and V. L. Tesh.** 1998. Shiga toxin type 1 activates tumor necrosis factor-α gene transcription and nuclear translocation of the transcriptional activators nuclear factor-κB and activator protein-1. Blood **92:**558–566.
36. **Sandvig, K., S. Grimmer, S. U. Lauvrak, M. L. Torgersen, G. Skretting, B. van Deurs, and T. G. Iversen.** 2002. Pathways followed by ricin and Shiga toxin into cells. Histochem. Cell Biol. **117:**131–141.
37. **Saxena, S. K., A. D. O'Brien, and E. J. Ackerman.** 1989. Shiga toxin, Shiga-like toxin II variant and ricin are all single-site RNA *N*-glycosidases of 28S RNA when microinjected into *Xenopus* oocytes. J. Biol. Chem. **264:**596–601.
38. **Shukaliak, J. A., and K. Dorovini-Zis.** 2000. Expression of the beta chemokines RANTES and MIP-1beta by human brain microvessel endothelial cells in primary culture. J. Neuropathol. Exp. Neurol. **59:**339–352.
39. **Siegler, R. L.** 1994. Spectrum of extrarenal involvement in postdiarrheal hemolytic-uremic syndrome. J. Pediatr. **125:**511–518.
40. **Slutsker, L., A. A. Ries, K. D. Greene, J. G. Wells, L. Hutwagner, and P. M. Griffin.** 1997. *Escherichia coli* O157:H7 diarrhea in the United States: clinical and epidemiologic features. Ann. Intern. Med. **126:**505–513.
41. **te Loo, D. M. W. M., L. A. H. Monnens, T. J. A. M. van der Velden, M. A. Vermeer, F. Preyers, P. N. M. Demacker, L. P. W. J. van den Heuvel, and V. W. M. van Hinsbergh.** 2000. Binding and transfer of verocytotoxin by polymorphonuclear leukocytes in hemolytic uremic syndrome. Blood **95:** 3396–3402.
42. **Tesh, V. L.** 1998. Cytokine response to Shiga toxins, p. 226–235. *In* J. B. Kaper and A. D. O'Brien (ed.), *Escherichia coli* O157:H7 and other Shiga toxin-producing *E. coli* strains. ASM Press, Washington, D.C.
43. **Tesh, V. L., J. A. Burris, J. W. Owens, V. M. Gordon, E. A. Wadolkowski, A. D. O'Brien, and J. E. Samuel.** 1993. Comparison of the relative toxicities of Shiga-like toxins type I and type II for mice. Infect. Immun. **61:**3392–3402.
44. **Tesh, V. L., J. E. Samuel, L. P. Perera, J. B. Sharefkin, and A. D. O'Brien.** 1991. Evaluation of the role of Shiga and Shiga-like toxins in mediating direct damage to human vascular endothelial cells. J. Infect. Dis. **164:**344–352.
45. **Thorpe, C. M., B. P. Hurley, L. L. Lincicome, M. S. Jacewicz, G. T. Keusch, and D. W. K. Acheson.** 1999. Shiga toxins stimulate secretion of interleukin-8 from intestinal epithelial cells. Infect. Immun. **67:**5985–5993.
46. **Thorpe, C. M., W. E. Smith, B. P. Hurley, and D. W. K. Acheson.** 2001. Shiga toxins induce, superinduce, and stabilize a variety of C-X-C chemokine mRNAs in intestinal epithelial cells, resulting in increased chemokine expression. Infect. Immun. **69:**6140–6147.
47. **Tsuchiya, S., M. Yamabe, Y. Yamaguchi, Y. Kobayashi, T. Konno, and K. Tada.** 1980. Establishment and characterization of a human acute monocytic leukemia cell line (THP-1). Int. J. Cancer **26:**171–176.
48. **van der Kar, N. C. A. J., L. A. H. Monnens, M. A. Karmali, and V. W. M. van Hinsbergh.** 1992. Tumor necrosis factor and interleukin-1 induce expression of the verocytotoxin receptor globotriaosylceramide on human endothelial cells: implications for the pathogenesis of the hemolytic uremic syndrome. Blood **80:**2755–2764.
49. **van Setten, P. A., L. A. H. Monnens, R. G. G. Verstraten, L. P. W. J. van den Heuvel, and V. W. M. van Hinsbergh.** 1996. Effects of verocytotoxin-1 on nonadherent human monocytes: binding characteristics, protein synthesis, and induction of cytokine release. Blood **88:**174–183.
50. **van Setten, P. A., V. W. M. van Hinsbergh, L. P. W. J. van den Heuvel, F. Preyers, H. B. P. M. Dukman, K. J. M. Assmann, T. J. A. M. van der Velden, and L. A. H. Monnens.** 1998. Monocyte chemoattractant protein-1 and interleukin-8 levels in urine and serum of patients with hemolytic uremic syndrome. Pediatr. Res. **43:**759–767.
51. **van Setten, P. A., V. W. M. van Hinsbergh, T. J. A. M. van der Velden, N. C. A. J. van de Kar, M. Vermeer, J. D. Mahan, K. J. M. Assmann, L. P. W. J. van den Heuvel, and L. A. H. Monnens.** 1997. Effects of TNF-α on verocytotoxin cytotoxicity in purified human glomerular microvascular endothelial cells. Kidney Int. **51:**1245–1256.
52. **Wozniak, A., W. H. Betts, G. A. Murphy, and M. Rokicinski.** 1993. Interleukin-8 primes human neutrophils for enhanced superoxide anion production. Immunology **79:**608–615.
53. **Yamasaki, C., Y. Natori, X.-T. Zeng, M. Ohmura, S. Yamasaki, Y. Takeda, and Y. Natori.** 1999. Induction of cytokines in a human colon epithelial cell line by Shiga toxin 1 (Stx1) and Stx2 but not by a nontoxic mutant Stx1 which lacks *N*-glycosidase activity. FEBS Lett. **442:**231–234.

Editor: A. D. O'Brien